Appl Water Sci (2017) 7:2727–2736
DOI 10.1007/s13201-016-0491-3

ORIGINAL ARTICLE

Biosorption of formic and acetic acids from aqueous solution using activated carbon from shea butter seed shells

Folahan A. Adekola[1] · **Ismaila A. Oba**[1]

Received: 21 December 2015 / Accepted: 11 October 2016 / Published online: 28 October 2016

Abstract The efficiency of prepared activated carbon from shea butter seed shells (SB-AC) for the adsorption of formic acid (FA) and acetic acid (AA) from aqueous solution was investigated. The effect of optimization parameters including initial concentration, agitation time, adsorbent dosage and temperature of adsorbate solution on the sorption capacity were studied. The SB-AC was characterized for the following parameters: bulk density, moisture content, ash content, pH, Fourier transform infrared spectroscopy (FTIR) and scanning electron microscopy (SEM). The optimal conditions for the adsorption were established and the adsorption data for AA fitted Dubinin–Radushkevich (D–R) isotherm well, whereas FA followed Langmuir isotherm. The kinetic data were examined. It was found that pseudo-second-order kinetic model was found to adequately explain the sorption kinetic of AA and FA from aqueous solution. It was again found that intraparticle diffusion was found to explain the adsorption mechanism. Adsorption thermodynamic parameters were estimated and the negative values of ΔG showed that the adsorption process was feasible and spontaneous in nature, while the negative values of ΔH indicate that the adsorption process was exothermic. It is therefore established that SB-AC has good potential for the removal of AA and FA from aqueous solution. Hence, it should find application in the regular treatment of polluted water in aquaculture and fish breeding system.

Keywords Adsorption · Wastewater · Formic acid · Acetic acid · Activated carbon

Introduction

The progressive increase of industrial technology results in relative increase in environmental pollution and a great effort has been made to minimize hazardous pollutants and, hence, avoiding their dangerous effects on animals, plants and humans (Nwabanne and Igbokwe 2012). Water pollution represents a great challenge and activated carbon is a common adsorbent used to remove hazardous contaminants from wastewater. The presence of formic acid and acetic acid in industrial effluents poses a serious environmental problem. The major ill effects caused by these acids are formation of kidney stones, vomiting and general body weakness (Kannan and Xavier 2001; Freitas et al. 2007). Thus, it is imperative that they are removed from industrial wastes before discharging them into the water body. Many techniques have been used in the past for the treatment of wastewater containing these pollutants, but proved ineffective. Adsorption is an effective technique for the removal of the dissolved pollutants (organic or inorganic) from water. Among many types of adsorbents, activated carbons are the most widely used, because of their large adsorptive capacity and low cost. Among the possible techniques for water treatments, the adsorption process by solid adsorbents shows potential as one of the most efficient methods for the treatment and removal of organic contaminants in wastewater treatment (Benkhedda et al. 2000). The adsorption capacity

Electronic supplementary material The online version of this article (doi:10.1007/s13201-016-0491-3) contains supplementary material, which is available to authorized users.

✉ Ismaila A. Oba
obaismail2012@gmail.com

Folahan A. Adekola
faadekola@yahoo.fr

[1] Department of Industrial Chemistry, University of Ilorin, Ilorin P.M.B. 1515, Kwara State, Nigeria

of activated carbon is linked to the large surface area, high microporosity and a high degree of surface reactivity (Khah and Ansari 2009). The main objective of this study is to investigate the potential use of activated carbon from shea butter seed shells, an agricultural waste material as a low-cost bio-adsorbent for removal of FA and AA from aqueous solution.

Materials and methods

Adsorbent preparation

Shea butter seed shells were obtained from shea butter trees within the University of Ilorin campus, Nigeria. The deseeded shea butter seed shells were washed several times, sun dried, chopped into small pieces and pyrolyzed at 500 °C for 30 min. The carbonized materials were allowed to cool to room temperature, crushed into a powder with the aid of a mortar and pestle and sieved with standard sieve of size $Ø < 90$ µm. The carbonized powdered sample obtained was washed with de-ionized water, filtered and dried in the oven at 105 °C. The purified activated carbon obtained was chemically activated by 1.0 M HNO_3 solution (Adegoke and Adekola 2010): 40 g of carbon sample was contacted with 400 mL of 1 M solution of HNO_3 at 140 °C and stirred for 2 h. Thereafter, it was washed several times to obtain neutrality with de-ionized water, filtered and dried again in the oven at 105 °C.

Characterization of activated carbon

The activated carbon was characterized for some physico-chemical properties such as ash content, moisture content, bulk density, iodine number and pH, which were determined in accordance with the standard methods of the American Society for Testing of Materials (ASTM) (Verla et al. 2012). Its surface morphology was characterized by scanning electron microscopy (SEM) (SEM-3020 ASPEX) and Fourier transform infrared (FTIR) spectroscopy before and after the uptake of FA and AA using a SHIMADZU 8400S Spectrometer for functional groups between 4000 and 500 $cm^{-1.}$

Adsorption experiments

The adsorption of AA and FA from aqueous solution by activated carbon was carried out using the batch technique. This involved the preparation of each adsorbate solution with different initial concentrations ranging from 0.2 to 1.0 mol L^{-1}. A known mass of adsorbent ranging from 20 to 100 mg was added to the different 250 mL conical flasks that contained 20 mL solution of each adsorbate and the mixture was agitated at 160 rpm on the mechanical shaker for varying times of 5–360 min and at varying temperatures of 30–60 °C. Thereafter, the mixture was filtered and the filtrate was analyzed by the potentiometric titration method. The quantity of each adsorbate adsorbed, Q_e (g g^{-1}), was calculated using the equation below:

$$Q_e = \frac{(C_o - C_e)V}{W},$$

where C_o and C_e are the initial and final concentrations (mol L^{-1}), respectively, W is the adsorbent dosage (g) and V is the volume of the solution (mL). The percentage (%) adsorbed was also calculated using the equation below (Itodo et al. 2009):

$$\%\text{adsorbed} = \frac{C_o - C_e}{C_o} \times 100.$$

Results and discussion

The summary of the proximate analysis of SB-AC is shown in Table 1.

Physicochemical characteristics of SB-AC

The FT-IR technique is an important tool to identify the characteristic functional groups on the adsorbent surface which in some cases are responsible for the binding of the adsorbate molecules (Salman et al. 2011). The FT-IR spectra of the chemically activated carbon from shea butter seed shells before and after adsorption are shown in Fig. 1a–c. The broad bands in the region 3414.12, 3437.26 and 3423.76 cm^{-1} before and after adsorption of FA and AA, respectively, were due to the hydroxyl stretching vibration, and the band in the region of 2924.18 cm^{-1} in the case of acetic acid was due to CH_2 asymmetric and symmetric stretching vibration. The stretching vibration of the C=O is at 1714.77 cm^{-1} for FA. The sharp peak at 2362.88 cm^{-1} before adsorption was slightly changed to 2359.02 cm^{-1} after adsorption of both FA and AA which was an evidence of the carbonyl group. The stretching

Table 1 Proximate analysis of SB-AC

Parameter	Value
pH	6.401
Ash content (%)	0.7
Moisture content (%)	1.2
Bulk density (g cm^{-3})	0.9077
Iodine number (mg g^{-1})	198.90

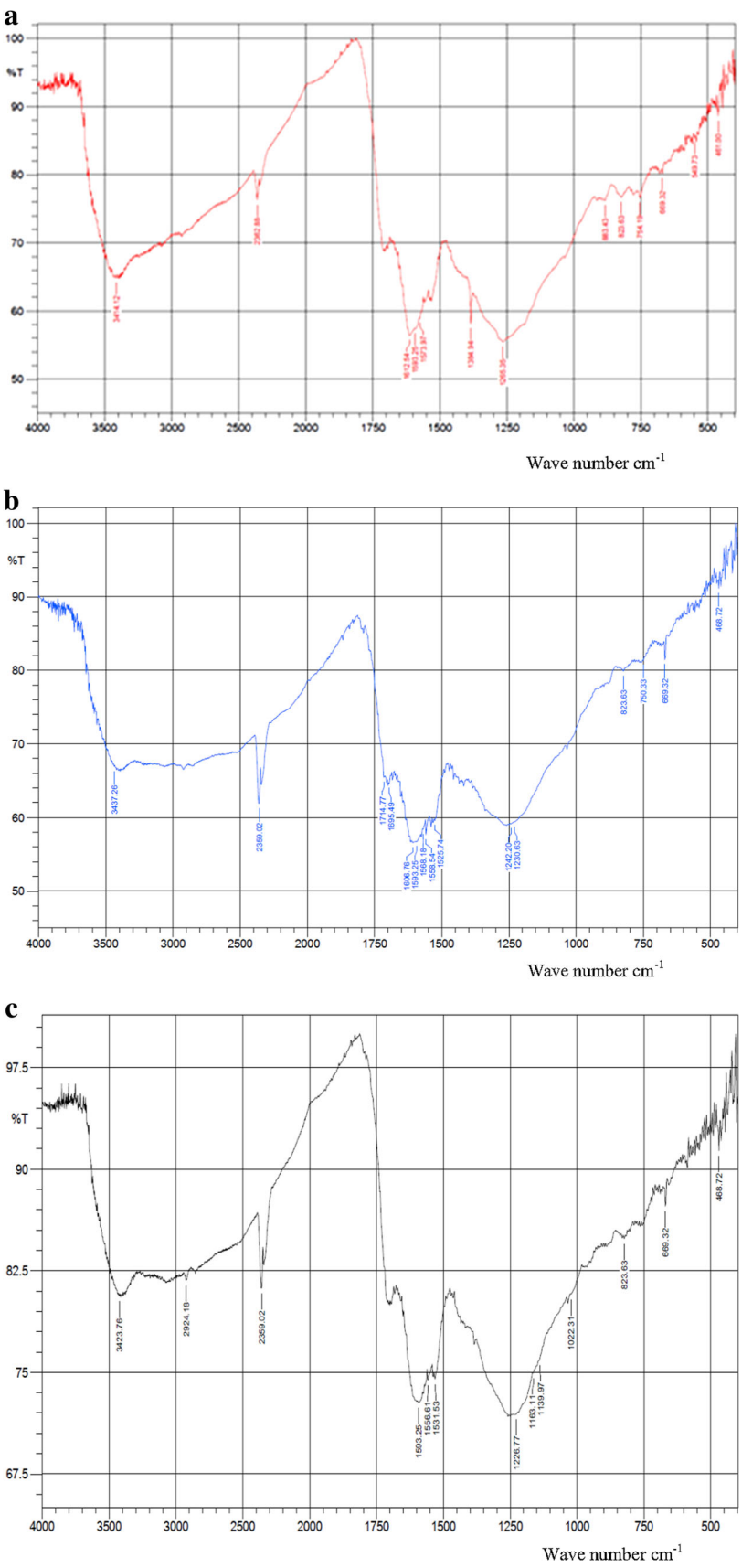

Fig. 1 **a** The FTIR spectrum of SB-AC before adsorption. **b** The FTIR spectrum of SB-AC after adsorption of formic acid. **c** The FTIR spectrum of SB-AC after adsorption of acetic acid

vibration of the COO− group lies between 1500 and 1600 cm^{-1}. The peaks at 1265.55, 1242.20 and 1226.77 cm^{-1} indicate the stretching vibration of C–O.

Scanning electron microscopy (SEM)

Scanning electron microscopy produces images of a sample by scanning it with a focused beam of electrons. The SEM images of the prepared activated carbon for both before and after adsorption of FA and AA are shown in Fig. 2.

Figure. 2a shows the morphology of SB-AC before adsorption. The carbon revealed that the surface of SB-AC was highly porous in nature and would enhance the adsorption of FA and AA. The carbon exhibited irregular net-like structure, which implied the formation of complete three-dimensional porous inner structures consisting of a rough surface area. The pore development in the char during pyrolysis was also important, as this would enhance the surface area and pore volume of the activated carbon by promoting the diffusion of the activating agent (HNO_3) molecules into the pores and thereby increasing the HNO_3–carbon interaction that create more pores on the surface of activated carbon. The development of these pores on the surface of SB-AC could be the main factor that led to the high uptake of AA and FA from aqueous solution. It is obvious in Fig. 2b, c that the large pores on the surface of activated carbon before adsorption were reduced after adsorption of adsorbate on the surface of carbon. This implied that formic acid and acetic acid were adsorbed onto the surface of the prepared activated carbon.

Effect of initial concentration

The initial concentration provides an important driving force to overcome all mass transfer resistance of FA and AA between the aqueous and solid phase. In the present study, the effect of initial concentration of acids on the adsorption by SB-AC was studied at a temperature of 30 ± 2 °C, 0.04 g adsorbent dose and 120 min contact time as clearly shown in Fig. 3a, b. The initial concentration of FA and AA increased from 0.2 to 1.0 mol L^{-1}. Figure 3a shows that the uptake of FA adsorption increased from 1.1646 to 1.8113 g g^{-1} with a decrease in percentage from 25.30 to 7.87%. Figure. 3b shows that the uptake of AA increased from 0.66055 to 4.56300 g g^{-1} with an increase in the initial concentration up to 0.8 mol L^{-1}. Then, the uptake decreased as the initial AA concentration further increased. The maximum percentage adsorption also increased from 11 to 20%. The reason may be that there exists a reduction in immediate solute adsorption owing to lack of active sites required for a high initial concentration of acid.

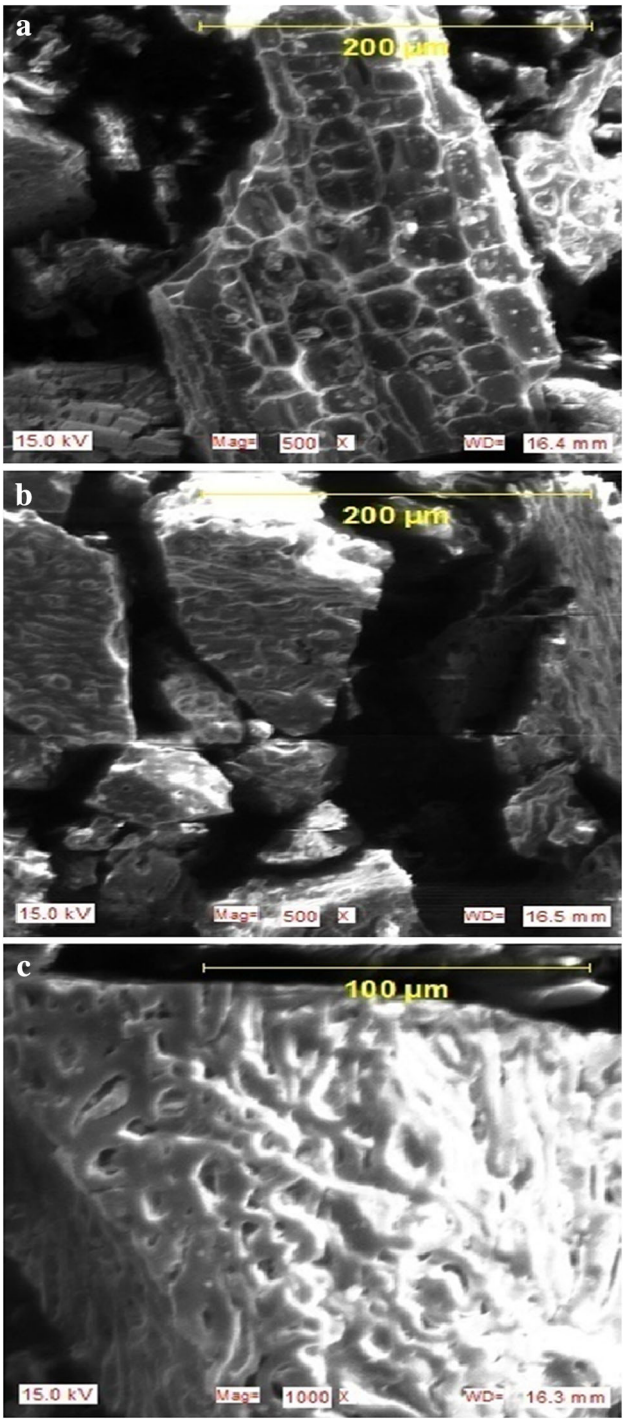

Fig. 2 **a** SEM image of SB-AC before adsorption. **b** SEM image of SB-AC after adsorption of FA. **c** SEM image of SB-AC after adsorption of AA

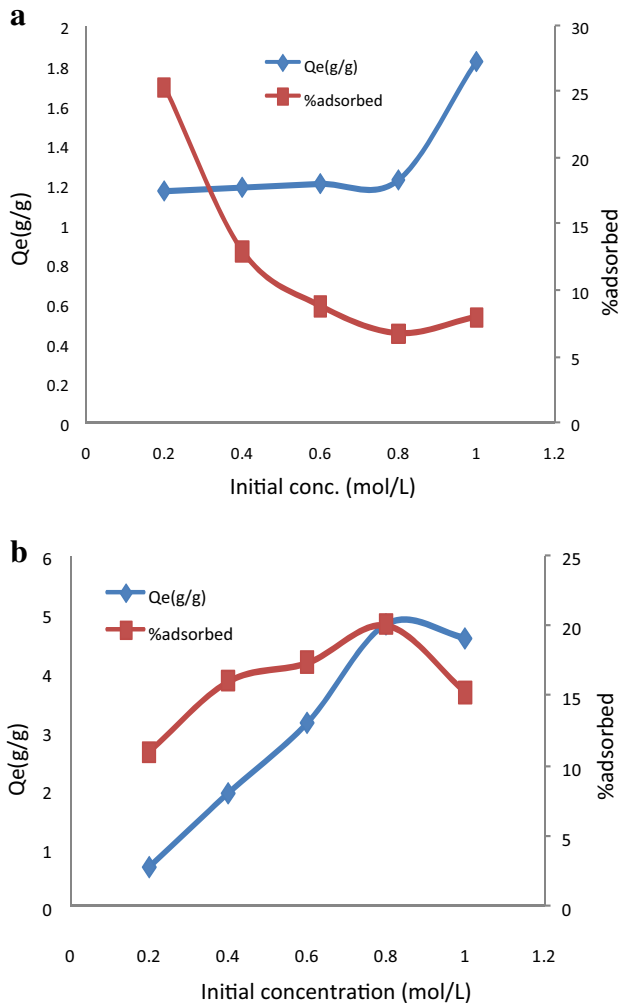

Fig. 3 **a** Effect of the initial concentration of FA. **b** Effect of initial concentration of AA

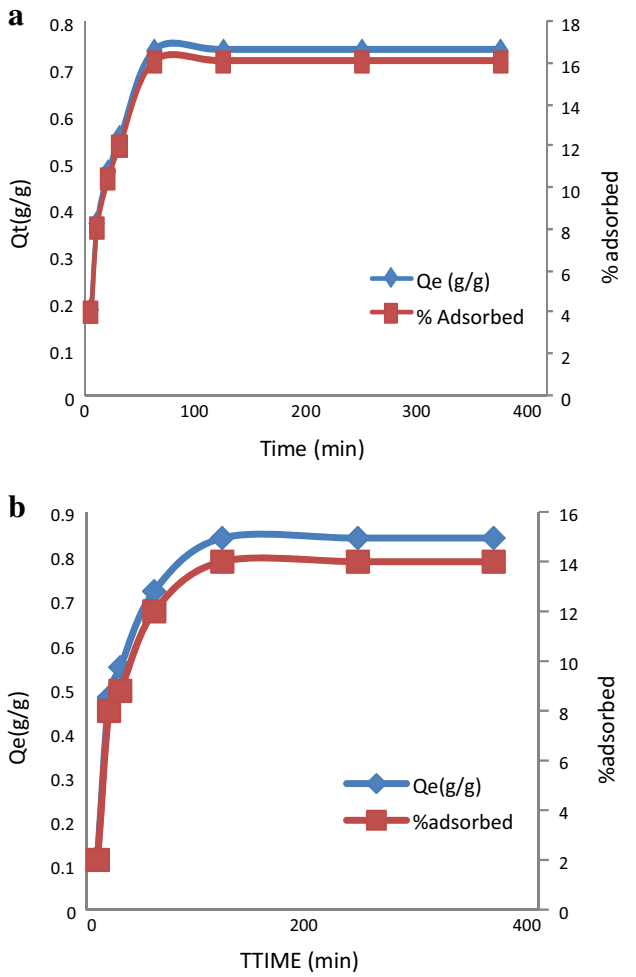

Fig. 4 **a** Effect of contact time on the adsorption of FA. **b** Effect of contact time on the adsorption of AA

Effect of contact time

Contact time is an important parameter to determine the equilibrium time of the adsorption process. The FA and AA uptakes by SB-AC are shown in Fig. 4a, b as a function of varying contact time from 5 to 360 min, at a fixed initial concentration of 0.2 and 0.8 mol L^{-1} FA and AA, respectively, 30 ± 2 °C temperature and 0.04 g adsorbent dose. It is obvious from Fig. 4a, that the adsorption capacity of FA increased from 0.18412 to 0.73648 g g^{-1} with increasing contact time. Large amounts of FA were removed in the first 30 min and equilibrium was reached at 60 min. After the equilibrium, adsorption uptake did not increase significantly. Further increase in contact time did not increase the uptake due to deposition of FA on the available adsorption site on the adsorbent material. At this point, the amount of the FA desorbing from the adsorbent is in a state of dynamic equilibrium with the amount of the FA being adsorbed onto the adsorbent. The time required to attain this state of equilibrium is 60 min, which is termed the optimum equilibrium time, and the amount of FA adsorbed at the equilibrium time reflects the maximum adsorption capacity of the adsorbent under those operating conditions. Similarly, Fig. 4b shows that in the first 20 min, the percentage removal of AA from aqueous solution increased rapidly from 2 to 15% and decreased thereafter which then increased slowly until optimum time was reached at 120 min for the adsorbate and subsequently became constant. The result indicates that the rate of adsorption of AA became higher during the initial time of adsorption and then lowers in the latter half of the process. This was due to the nature of the adsorbent and the available adsorption sites, which affect the rate of adsorption of the adsorbate. This difference in the rate of adsorption may be due to the fact that initially, all adsorbent sites were vacant so the adsorption was high. Later, due to the decrease in the number of adsorption sites on the adsorbent, as well as concentration of adsorbates in the

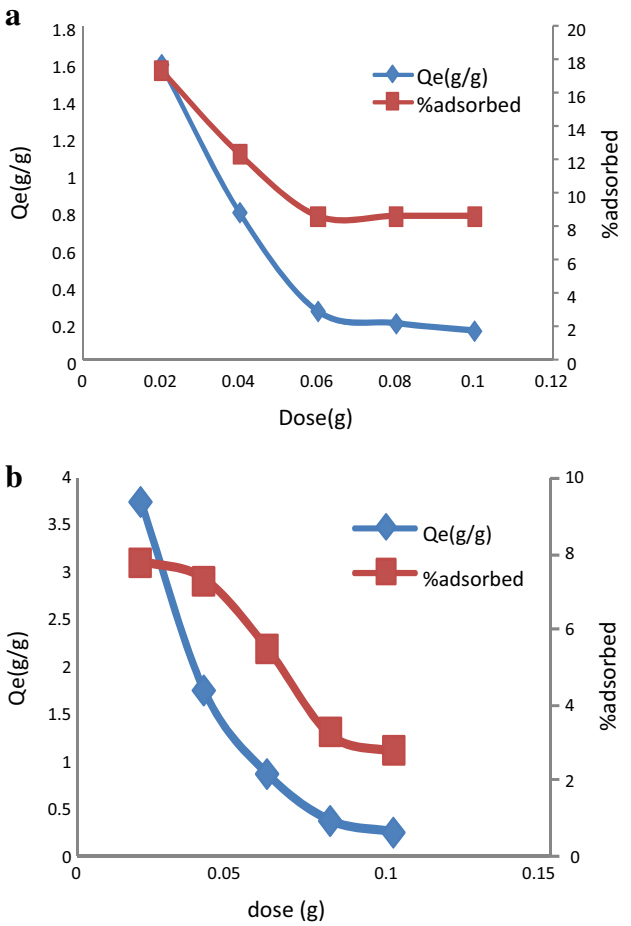

Fig. 5 **a** Effect of adsorbent dose on the adsorption of FA. **b** Effect of adsorbent dose on the adsorption of AA

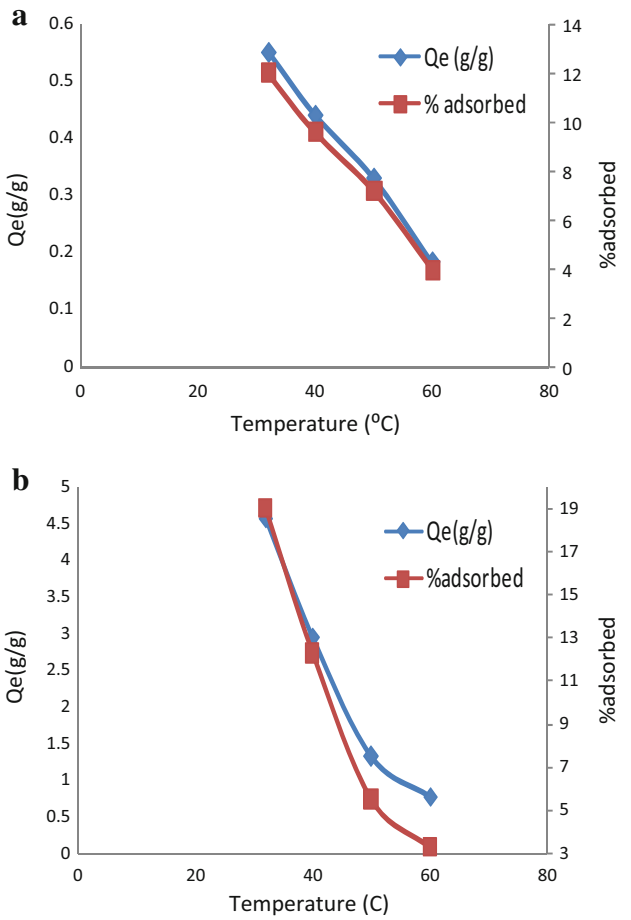

Fig. 6 **a** Effect of temperature on the adsorption of FA. **b** Effect of temperature on the adsorption of AA

solution, the adsorption became slow. Similar results have been reported for the removal of carboxylic acids on fly ash and activated carbons. Furthermore, the remaining vacant surface sites were difficult to be occupied due to the repulsive forces, as well as the competition between adsorbate molecules on the adsorbent surface (Srivastava et al. 2006).

Effect of dosage

The effect of the adsorbent dose determines the capacity of the adsorbent for a given FA and AA concentration. In this study, the effect of adsorbent dose on the extent of solutes adsorption was investigated by varying the dosage from 0.02 to 0.1 g for SB-AC, at 0.2 and 0.8 mol L^{-1} fixed initial concentration of FA and AA, respectively, 120 min contact time and 30 ± 2 °C temperature. Figure 5a, b shows the plots of the FA and AA uptake against the quantity of the adsorbent, respectively. FA and AA uptake per unit mass decreased from 1.5972 to 0.1593 g g^{-1} and 3.72310 to 0.26902 g g^{-1}, respectively, with the increase in the adsorbent dosage from 0.02 to 0.1 g. The reason for this trend may be attributed to the fact that at high adsorbent dosages, the available FA and AA molecules are not able to cover all the available sites on the adsorbents, resulting in low uptake.

Effect of temperature

Temperature has an important effect on the process of adsorption. The effect of temperature on the removal of FA and AA from aqueous solution was investigated by varying the temperature ranging from 30 to 60 °C under optimized conditions of 0.04 g adsorbent dose and 120 min contact time at fixed initial concentration of 0.2 mol L^{-1} for FA and 0.8 mol L^{-1} for AA. These are depicted in Fig. 6a, b. The adsorption of FA and AA decreased from 0.55236 to 0.18412 g g^{-1} and from 4.5638 to 0.78065 g g^{-1}, respectively, as temperature increased. This can be explained by the exothermic spontaneity of the adsorption process. The

attractive forces between the adsorbent and adsorbate ions may have been weakened to decreasing the adsorption. At high temperature, the thickness of the boundary layer is expected to decrease due to the increased tendency of the ions to escape from the surface of the adsorbent to the solution phase and hence this is bound to weaken the adsorption interactions between the adsorbent and the adsorbates.

Adsorption isotherms

The adsorption data were analyzed with some isotherms at the following experimental conditions: $C_o = 0.8$ mol L^{-1} for AA and 0.2 mol L^{-1} for FA, $W = 0.04$ g, temperature = 32 °C and 120 min at 160 rpm. The adsorption isotherm is a fundamental concept in adsorption science. It is the equilibrium relationship between the amount of the substance adsorbed and its concentration in the bulk fluid phase at a constant temperature. The primary experimental information is usually made up of these isotherms, commonly used as a tool to distinguish among different adsorbents and by this means selecting the fitting ones for a particular application (Srivastava et al. 2006). Several models are available in literature to describe the experimental data of the adsorption isotherm. In the current study, 2 parameter isotherms proposed by Freundlich, Langmuir and Temkin and 3 parameter isotherms proposed by Dubinin–Radushkevitch (D–R) were examined with the equilibrium data obtained from the experiments. The fitted parameters for 2 and 3 parameter models, as well as the correlation coefficient (R^2), are summarized in Table 2.

Table 2 Parameters of Freundlich, Langmuir, Dubinin–Radushkevich (D–R) and Temkin isotherm model for adsorption of FA and AA onto SB-AC

Isotherms	Parameters	Values	
		FA	AA
Freundlich	n	6.25	0.7657
	K_f (mol g^{-1})	0.031989	0.11995
	R^2	0.381	0.954
Langmuir	Q_o (g g^{-1})	0.03897	0.14376
	K_L (L mol^{-1})	5.91762	0.47939
	R^2	0.822	0.362
Temkin	B (J mol^{-1})	0.005	0.046
	A_T	601.845	6.774
	R^2	0.364	0.932
D–R	B_D (mol^2 kJ^{-2})	3×10^{-12}	1×10^{-7}
	q_s (g g^{-1})	1.38127	7.5007
	E (kJ mol^{-1})	12.91	2.2361
	R^2	0.162	0.985

The high value of R^2 (close or equal 1) indicates the conformity among experimental data with the model isotherm.

The adsorption constants of a given isotherm allow, not only to evaluate the adsorbent properties of a sample, but also to determine if adsorption is favorable or not. The values of the constants for Langmuir, Freundlich, D–R and Temkin isotherm models at 305 °K for the removal of AA and FA onto SB-AC are presented in Table 2 above. For the adsorption of AA onto SB-AC, the R^2 value obtained from the D–R model was the highest when compared with those of the Langmuir, Freundlich and Temkin models. Therefore, the D–R model is the most suitable and the order of fitting of the isotherms can be ranked: D–R > Freundlich > Temkin > Langmuir adsorption models. This is a sign of a strong interaction between AA and SB-AC. Langmuir isotherm model appears to be a fairly good model for the adsorption of FA onto SB-AC due to its high regression coefficient ($R^2 = 0.822$). The constant of Langmuir (K_L) measures the intensity of adsorption. In fact, the higher the K_L value, the stronger is the affinity between the adsorbate and adsorbent. The D–R model gives information on the binding energies. The average free energy, E, of a molecule of adsorbent expresses the energy released when a molecule of adsorbate passes from the solution into the adsorbent (Kilic et al. 2011). It can be observed from Table 2 that the sorption of AA onto SB-AC is governed by physical adsorption mechanisms, since $E < 8$ kJ mol^{-1} (Ansari and Mosayebzadeh 2010), while that of FA onto SB-AC is governed by chemical adsorption mechanisms since $E > 8$ kJ mol^{-1} (Ansari and Mosayebzadeh 2010).

Adsorption kinetics and mechanism

To study the kinetic models for the adsorption of AA and FA on SB-AC, pseudo-first-order, pseudo-second-order and Elovich models were used, while the adsorption mechanism was evaluated by the intraparticle diffusion model. The plots of all the kinetic models used in this work are depicted in Fig. 7 and their kinetic parameters calculated from the slope and intercept of each plot and summarized in Table 3 under the following experimental conditions: initial conc. of FA and AA are 0.2 and 0.8 mol L^{-1} respectively, adsorbent dose (W) = 0.04 g, temperature = 30 ± 2 °C and contact time = 120 min at 160 rpm.

It is evident from Table 3 that the pseudo-second-order kinetic model has the highest regression correlation coefficient ($R^2 = 0.996$) for FA and $R^2 = 0.952$ for AA when compared with those obtained from the pseudo-first-order and Elovich model. This implied that the pseudo-second-order model adequately gave the best description of the

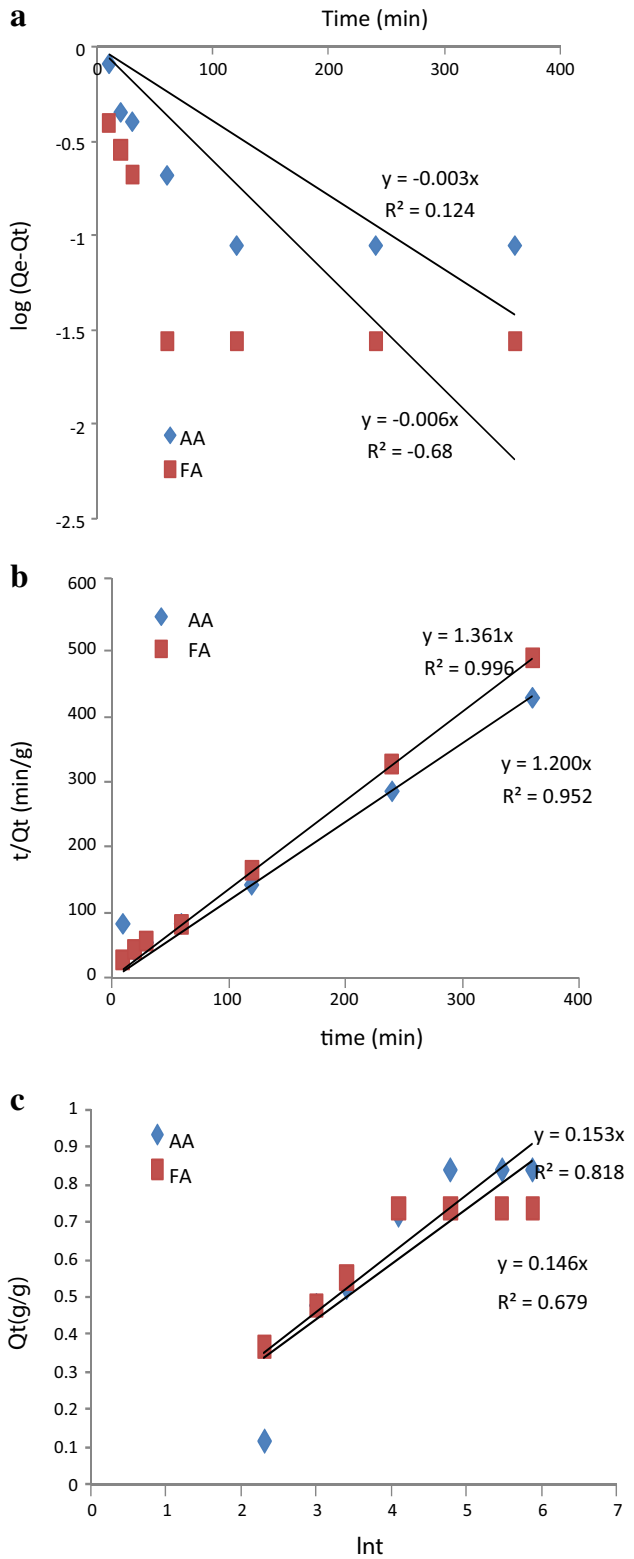

Fig. 7 Pseudo-first-order **(a)**, Pseudo-second-order **(b)** and Elovich **(c)** kinetic plots

Table 3 Pseudo-first-order, pseudo-second-order and Elovich kinetic data

Kinetic model	Parameters	Values	
		FA	AA
Pseudo-first order	K_1 (min^{-1})	1.342×10^2	6.91×10^3
	Q_e, cal. (g g^{-1})	1.000	1.0
	R^2	−0.68	0.124
Pseudo-second order	K_2 (g g^{-1} min^{-1})	0	0
	Q_e, cal. (g g^{-1})	0.7348	0.833
	R^2	0.996	0.952
Elovich	A	0.146	0.153
	B	6.849	6.536
	R^2	0.679	0.818

adsorption kinetics of the two adsorbates from the aqueous solution. It is also pertinent to note the concordance between the experimental and theoretical values for AA (0.9302 and 0.833 g g^{-1}) and FA (0.7639 and 0.7348 g g^{-1}), respectively.

Adsorption mechanism

The Weber–Morris intraparticle diffusion model was used to determine whether the overall rate of adsorption was controlled by intraparticle diffusion, i.e., the movement of the adsorbate molecules into the interior of the adsorbent particles. A plot of q_t versus $t^{1/2}$ gives a linear relationship as shown in Fig. 8. The value of intercept (C) and the calculated value of intraparticle diffusion rate constants (Kid) from the slope are summarized in Table 4. The larger intercept values suggest that intraparticle diffusion has a lesser role to play compared with surface diffusion. The figure revealed that two steps occur in the adsorption process. The sharply rising part is the external surface adsorption stage, while the second linear part is the gradual adsorption stage where intraparticle or pore diffusion is rate limiting. The high R^2 values of the sharply rising part suggest that the external surface adsorption is the rate-limiting step. The deviation of the lines from the origin and the low R^2 values of the gradual adsorption stage suggest that intraparticle diffusion is not the sole rate-limiting step, as a similar result was earlier reported. This implied that the external surface adsorption or instantaneous adsorption stage occurred and could be used to describe the mechanism of the adsorption process (Theivarasu et al. 2011).

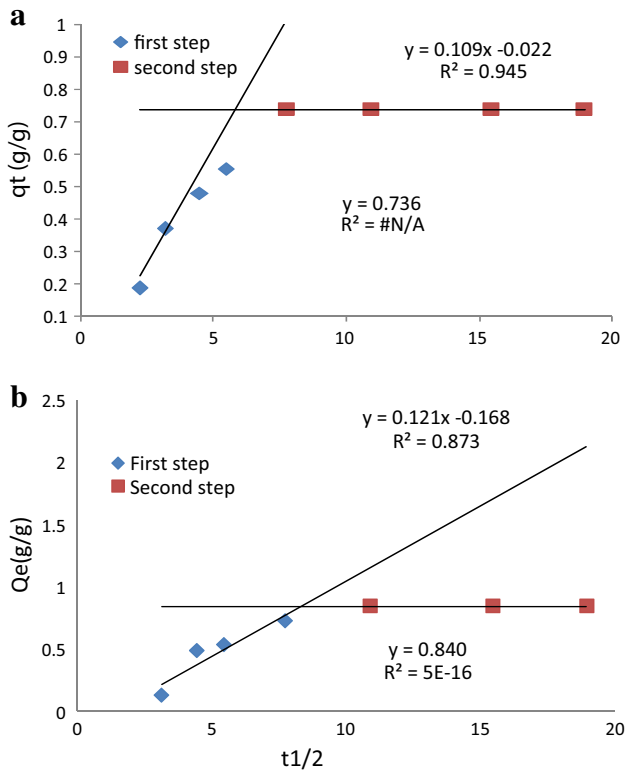

Fig. 8 Intraparticle diffusion plot for FA **(a)** and intraparticle diffusion plot for AA **(b)**

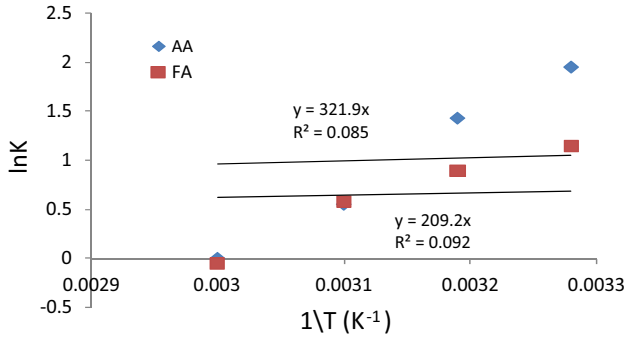

Fig. 9 Van't Hoff plots

Adsorption thermodynamics

The values of these parameters (ΔH°, ΔS°, ΔG°) for the adsorption of adsorbates (AA and FA) onto adsorbent are listed in Table 5. The changes in enthalpy (ΔH) and entropy (ΔS) are negative. This implies that the reaction was exothermic, being unfavorable at higher temperatures. This is clear from the effect of temperature results as shown in Fig. 9. Decrease in adsorption with increase in temperature has been attributed to the weakening of adsorptive forces between the active sites of the adsorbent and adsorbate species and also between adjacent molecules on the adsorbed phase. The values of the adsorption entropy change (ΔS°) are negative, which indicate that the mobility of adsorbates on the surface of the adsorbent is more restricted as compared to those in solution. The negative values of the adsorption free energy (ΔG°) in Table 5 demonstrated that the adsorption was spontaneous. The thermodynamic results obtained in this study were in agreement with those observed by other researchers (Mane et al. 2007; Pan et al. 2003).

Conclusion

The shea butter seed shells activated carbon (SB-AC) was found to be an effective adsorbent for the removal of formic acid and acetic acid from aqueous solution. The study showed that the initial concentration, contact time, the adsorbent dose and temperature of the solution influenced the adsorption process. Thermodynamic studies showed that the adsorption process was feasible, spontaneous and exothermic in nature. Langmuir isotherm best fitted the data for FA which confirmed the monolayer adsorption,

Table 4 Intraparticle diffusion model

FA				AA		
Step	Kid (mg g^{-1} $min^{-1/2}$)	C	R^2	Kid (mg g^{-1} $min^{-1/2}$)	C	R^2
1	0.109	−0.022	0.945	0.121	−0.168	0.873

Table 5 The thermodynamic parameters (ΔH, ΔS and ΔG) evaluated from the Van't Hoff plot

Adsorbate	ΔG (kJ mol^{-1})				ΔH (kJ mol^{-1})	ΔS (kJ mol^{-1} K^{-1})
	305 (K)	313 (K)	323 (K)	333 (K)		
FA	−3.0784	−2.2469	−1.2076	−0.1683	−34.7770	−0.1039
AA	−5.005	−3.5666	−1.7686	−0.0294	−59.8440	−0.1798

while sorption of AA followed Dubinin–Radushkevich (D–R) model which gave information on binding energy. The adsorption of both adsorbates followed pseudo-second-order rate kinetics. Therefore, the use of SB-AC as low-cost bio-sorbent is recommended for the adsorption of other carboxylic acids from aqueous solution.

References

Adegoke HI, Adekola FA (2010) Removal of phenol from aqueous solution by activated carbon prepared from some agricultural materials. Adv Nat Appl Sci 4(3):293–298 (**ISSN 1995-0748**)

Ansari R, Mosayebzadeh Z (2010) Removal of basic dye methylene blue from aqueous solutions using sawdust and sawdust coated with polypyrrole. J Iran Chem Soc 7:339–350

Benkhedda J, Jaubert JN, Barth D, Perrin L, Baily M (2000) Adsorption isotherms of *m*-Xylene on activated carbon: measurements and correlation with different models. J Chem Thermodyn 32:401–411

Freitas AF, Mendes MF, Coelho GLV (2007) Thermodynamic study of fatty acids adsorption on different adsorbents. J Chem Thermodyn 39:1027–1037

Itodo AU, Abdulrahman FW, Hassan LG, Maigandi SA, Itodo HU (2009) Gas chromatographic prediction of equilibrium phase Atrazine after sorption onto derived activated carbon. Int J Poult Sci 8(12):1174–1182

Kannan N, Xavier A (2001) New comparative mixed adsorbents for the removal of acetic acid by adsorption form aqueous solutions. A Comp Study Toxical Env Chem 79(1):95–100

Khah M, Ansari R (2009) Activated charcoal: preparation, characterization and applications: a review article. Int J Chem Tech Res 1(4):859–864

Kilic M, Apaydin-Varol E, Putin AE (2011) Adsorptive removal of phenol from aqueous solutions on activated carbon prepared from tobacco residues, equilibrium, kinetics and thermodynamics. J Hazard Mater 189:397–403

Mane VS, Deo Mall I, Srivastava VC (2007) Kinetic and equilibrium isotherm studies for the adsorptive removal of Brilliant Green dye from aqueous solution by rice husk ash. J Env Manag 84(4):390–400

Nwabanne JT, Igbokwe PK (2012) Mechanism of copper (II) removal from aqueous solution using activated carbon prepared from different agricultural materials. Int J Multidiscip Sci Eng 3(7):46–52 [ISSN:2045-7057, **https://www.ijmse.org**]

Pan SC, Lin CC, Tseng DH (2003) Reusing sewage sludge ash as adsorbent for copper removal from wastewater. Resour Conserv Recy 39:79–90

Salman JM, Njoku VO, Hameed BH (2011) Batch and fixed-bed adsorption of 2,4-dichloro phenoxyacetic acid onto oil palm frond activated carbon. Chem Eng J 174:33–40

Srivastava VC, Swamy MM, Mall ID, Prasad B, Mishra IM (2006) Adsorptive removal of phenol by bagasse fly ash and activated carbon equilibrium, kinetics and thermodynamics. Colloids Surf A 272:89–104

Theivarasu C, Mylsamy S, Sivakumar N (2011) Cocoa shell as adsorbent for the removal of methylene blue from aqueous solution, kinetic and equilibrium study. Univers J Environ Res Technol 1:70–78

Verla AW, Horsfall M, Verla EN, Spiff AI, Ekpete OA (2012) Preparation and characterization of activated carbon from fluted pumpkin (*Telfairia occidentalis* Hook.F) seed shell. Asian J Nat Appl Sci 1(3):39–50